Published in final edited form as:
J Pathol. 2014 November ; 234(3): 375–385. doi:10.1002/path.4403.

NF-κB inducing kinase is a key regulator of inflammation-induced and tumor-associated angiogenesis

A.R. Noort[1,2], **K.P.M. van Zoest**[1,2], **E.M. Weijers**[3], **P. Koolwijk**[3], **C.X. Maracle**[1,2], **D.V. Novack**[4], **M.J. Siemerink**[5], **R.O. Schlingemann**[5], **P.P. Tak**[1,6,†], and **S.W. Tas**[1,2,*]

[1] Department of Clinical Immunology & Rheumatology, Academic Medical Center/University of Amsterdam, The Netherlands [2]Department of Experimental Immunology, Academic Medical Center/University of Amsterdam, The Netherlands [3]Department of Physiology, Institute for Cardiovascular Research (ICaR-VU), VU Medical Center, Amsterdam, The Netherlands [4] Division of Bone and Mineral Diseases, Departments of Medicine and Pathology, Washington University School of Medicine, St. Louis, Missouri, United States of America [5] Ocular Angiogenesis Group, Department of Ophthalmology and Department of Cell Biology and Histology, Academic Medical Center/University of Amsterdam, The Netherlands [6] Department of Medicine, University of Cambridge, Cambridge, United Kingdom

Abstract

Angiogenesis is essential during development and in pathological conditions such as chronic inflammation and cancer progression. Inhibition of angiogenesis by targeting vascular endothelial growth factor (VEGF) blocks disease progression, but most patients eventually develop resistance which may result from compensatory signaling pathways. In endothelial cells (EC) expression of the pro-angiogenic chemokine CXCL12 is regulated by non-canonical nuclear factor (NF)-κB signaling. Here, we report that NF-κB-inducing kinase (NIK) and subsequent non-canonical NF-κB signaling regulates both inflammation-induced and tumor-associated angiogenesis. NIK is highly expressed in endothelial cells (EC) in tumor tissues and inflamed rheumatoid arthritis synovial tissue. Furthermore, non-canonical NF-κB signaling in human microvascular EC significantly enhanced vascular tube formation, which was completely blocked by siRNA targeting NIK. Interestingly, $Nik^{-/-}$ mice exhibited normal angiogenesis during development and unaltererd TNFα- or VEGF-induced angiogenic responses, whereas angiogenesis induced by non-

*Corresponding author: S.W. Tas, MD/PhD, Department of Clinical Immunology & Rheumatology, Academic Medical Center/ University of Amsterdam, Meibergdreef 9, 1105AZ, Amsterdam, PO. Box 22600, The Netherlands, phone: +31 20 56 67765, fax: +31 20 6919658, S.W.Tas@amc.uva.nl.
†Current address also: GlaxoSmithKline, Stevenage, United Kingdom

Author contributions

A.R.N. contributed to the study design, all experiments, data analysis, and writing of the manuscript. K.P.M.Z. performed and collected data for in vitro and ex vivo experiments. E.M.W. contributed to the tube formation experiments and drafting of the manuscript. P.K. contributed to and provided materials for tube formations experiments, discussion, and drafting the manuscript. C.X.M. performed and collected data for in vitro and ex vivo experiments. M.J.S. performed and analysed data of retina experiments. R.O.S. provided materials, advice and contributed to drafting of the manuscript. D.V.N. performed and provided materials for in vivo experiments, discussion, and drafting of the manuscript. P.P.T. contributed to study design, drafting of the manuscript and provided advice and discussion. S.W.T. was responsible for project conceptualization, experimental design, writing of the manuscript and funding of the project.

Disclosure of conflicts of interest

The authors declare no competing financial interests.

canonical NF-κB stimuli was significantly reduced. In addition, angiogenesis in experimental arthritis and a murine tumor model was severely impaired in these mice. These studies provide evidence for a role of non-canonical NF-κB signaling in pathological angiogenesis, and identify NIK as a potential therapeutic target in chronic inflammatory diseases and tumor neoangiogenesis.

Keywords

NF-κB; endothelial cells; angiogenesis; inflammation; NIK

INTRODUCTION

Angiogenesis is defined as the formation of new blood vessels from the pre-existing vasculature. It is a highly coordinated process occurring both during normal development and in pathological conditions such as atherosclerosis, chronic inflammation and cancer [1]. Activation of endothelial cells (EC) is pivotal in this process and can result in the formation of new blood vessels, most notably via vascular endothelial growth factor (VEGF) receptor stimulation [2]. In chronic inflammation, including rheumatoid arthritis (RA), and in tumors, pathological angiogenesis occurs when activated stromal cells and inflammatory cells secrete pro-angiogenic factors like VEGF [2-4] that trigger quiescent EC to differentiate and form new blood vessels [1]. Importantly, inhibition of angiogenesis by targeting VEGF blocks disease progression in (pre-)clinical models of arthritis [5,6] and various cancers [7]. Anti-VEGF monoclonal antibodies are used in clinical practice for eye diseases with neovascularization and metastatic cancer. However, most patients develop resistance [8,9], which may result from compensatory signaling pathways [7]. These pathways can for instance induce inflammatory cytokines and proteases that contribute to enhanced angiogenesis in chronic inflammation and tumors [1].

Nuclear factor-κB (NF-κB) transcription factors can be activated via two distinct signaling pathways. The canonical NF-κB pathway is activated by pro-inflammatory stimuli such as TNFα, and requires inhibitor of κB (IκB) kinase (IKK)β, whereas IKKα is dispensable [10]. In contrast, the non-canonical pathway is strictly dependent on NF-κB-inducing kinase (NIK) and IKKα, but does not require IKKβ [11]. This pathway can be activated via TNF-receptor superfamily members such as the lymphotoxin β receptor (LTβR) and CD40 [10]. All known inducers of the non-canonical NF-κB pathway also stimulate canonical NF-κB activity [12].

In EC, the canonical NF-κB pathway is critical for pro-inflammatory gene expression, including TNFα [13,14]. Furthermore, VEGF-receptor signaling induces canonical NF-κB signaling in EC and VEGF gene expression is regulated in part via the canonical NF-κB pathway [15]. In contrast, the function of non-canonical NF-κB signaling in EC is largely unknown. CXCL12, an important chemokine for lymphocyte transendothelial migration with pro-angiogenic properties [16], is regulated by non-canonical NF-κB signaling in EC [17], and is expressed both in RA synovial tissue EC [18] and in cancer EC (reviewed in [19]). In lymphoid tissues, lymphotoxin (LT)β receptor dependent non-canonical NF-κB signaling is required for high endothelial venule (HEV) differentiation and function [20,21].

Interestingly, HEVs are also present in chronically inflamed tissues such as RA synovial tissue [22], and are also induced in tumors after antibody-LT fusion protein treatment [23]. In addition, LTβ and LIGHT (homologous to Lymphotoxins, exhibits Inducible expression, and competes with HSV Glycoprotein D for HVEM, a receptor expressed by T-lymphocytes), both ligands of the LTβR, and CD40L are expressed in RA synovial tissue [24-26]. Furthermore, LTβ and LIGHT are produced by host immune cells in tumors [27,28] and promote tumor growth [28,29]. Non-canonical NF-κB signaling in tumor cells is involved in tumor progression[30], but its contribution to angiogenesis has not been investigated yet.

Therefore, we investigated the role of non-canonical NF-κB signaling in inflammation-induced and tumor-associated angiogenesis, and compared this with its requirement for angiogenesis during development. In our studies we used human RA synovial tissue biopsies and various human cancer tissues, complemented with murine disease models in Nik−/− mice.

MATERIALS & METHODS

Human tissues

Synovial tissue biopsies were taken from knee joints of active RA patients or from healthy individuals. Early RA was defined as a disease duration of < 1 year and established RA as a disease duration of >2 years [31]. Tumor tissues were obtained from the department of pathology of the Academic Medical Center (AMC). All tissue collection was done at the AMC and approved by the Medical Ethical Commission.

Mice

$Nik^{-/-}$ mice (C57/Bl6 background) and Wt littermate controls were kindly provided by D.V. Novack (Washington University, St. Louis, MO) [32]. All experimental procedures were reviewed and approved by the experimental animal committee of the AMC.

Immunohistochemical staining

Frozen human tissue sections (synovial tissues, tumor tissues, or normal healthy tissues) were cut (5 μm) and mounted on Star Frost adhesive glass slides (Knittelgläser, Braunschweig, Germany). Sections were fixed with acetone and endogenous peroxidase activity was blocked with 0.3% H_2O_2 in 0.1% sodium azide in PBS. Sections were stained with monoclonal primary antibodies against NIK (sc-8417, Santa Cruz Biotechnology, Santa Cruz, CA), p52 (#4882, Cell Signaling technology, Danvers, MA) and CXCL12 (MAB350, R&D Systems, Abingdon, United Kingdom) and secondary antibodies goat-anti-mouse (p0447, DAKO, Glostrup, Denmark) or swine-anti-rabbit (p0399, DAKO) and streptavidin labeled with horseradish peroxidase. Biotinylated tyramine was used for amplification, as previously described [33]. As negative controls, sections were incubated with isotype control antibodies (all R&D Systems).

Immunofluorescence staining

Tissue sections were fixed with acetone and incubated with the following monoclonal mouse antibodies: anti-NIK (sc-8417, Santa Cruz Biotechnology); polyclonal goat antibodies: anti-CD31 (sc-1505, Santa Cruz Biotechnology), anti-CD34 (sc-7045, Santa Cruz Biotechnology); polyclonal rabbit antibodies: anti-IKKα (ab17943, Abcam, Cambridge, United Kingdom). For doublefluorescence stainings of NIK with CD31/34, slides were incubated with goat anti-mouse-HRP (p0447, DAKO), and subsequently incubated with streptavidine-Alexa-594 (S-32356, Molecular Probes Europe, Leiden, The Netherlands), Alexa-488-conjugated goat-anti-rabbit (A-11008, Molecular Probes Europe) and Alexa 488-conjugated rabbit-anti-goat (A-11034, Molecular Probes Europe). For doublefluorescence stainings of NIK with IKKα, slides were incubated with Alexa 594-conjugated goat-anti-Mouse (A-11005, Molecular Probes Europe) and Alexa-488-conjugated donkey-anti-rabbit (A-21206, Molecular Probes Europe). Slides were mounted with Vectashield containing DAPI (VC-H-1500, Brunschwig, Amsterdam, The Netherlands). Isotype control antibodies were used as negative control (all R&D Systems). Slides were analyzed using a Leica DMRA fluorescence microscope (Leica, Wetzlar, Germany) coupled to a CCD camera and Image-Pro Plus software (Dutch Vision Components, Breda, The Netherlands). A ratio of NIK pixel values to CD31/CD34 pixel values was calculated for each image (n=10) for determination of double-positive areas.

Human microvascular endothelial cell culture

Human microvascular endothelial cells (HMVEC) from foreskin were isolated and characterized as described previously [34]. HMVEC were cultured on gelatin-coated culture plates in Medium 199 supplemented with 100 U/ml penicillin, 100 mg/ml streptomycin (p/s), 2 mM L-glutamin (all Lonza, Verviers, Belgium), 5 U/ml heparin, 3.75 μg/ml EC growth factor (ECGF, crude extract from bovine brain), 10% heat-inactivated human serum (HSi, PAA Laboratories, Pasching, Austria) and 10% heat-inactivated newborn calf serum (NBCSi, Lonza). Confluent cells were trypsinized (0.05% trypsin in HBSS, both Lonza) and replated in a 1:3 density. Cells were used until passage 10.

In vitro tube formation assay

In vitro angiogenesis was determined with HMVEC in three-dimensional fibrin matrices, as described before [14]. Fibrin matrices were prepared by addition of thrombin (0.1 U/ml) to a 2 mg/ml fibrinogen solution (Kordia, Leiden, The Netherlands) in M199 medium (Invitrogen, Carlsbad, CA). After polymerization, thrombin was inactivated by adding M199 supplemented with p/s, 10% HSi and 10% NBCSi. HMVEC were seeded in confluent density on the fibrin matrices and after 24h, and subsequently at 48h intervals, HMVEC were incubated with M199, p/s, 10% HSi, 10% NBCSi, 10 ng/ml TNFα (Sigma-Aldrich, St Louis, MO) and 10 ng/ml fibroblast growth factor-2 (FGF-2, Preprotech, London, UK) in the presence or absence of 30 ng/ml lymphotoxin $\alpha_1\beta_2$ (LT; R&D Systems, Abingdon, United Kingdom), 30 ng/ml LIGHT (R&D Systems) or 30 ng/ml CD40L (Enzo Life Sciences, Antwerp, Belgium). The total length of formed tube-like structures from HMVEC into the fibrin matrices was analyzed by phase contrast microscopy and Optimas image analysis software [35]. Tube formation of HMVEC isolated from various donors was

determined in quadruplicate wells. HMVEC were transfected with siRNAs targeting NIK, IKKα, IKKβ, or a non-targeting siRNA (siGENOME SMARTpool, Dharmacon, Lafayette, CO) by using the AMAXA basic nucleofector kit for primary EC (Lonza), according to manufacturers protocols. Transfection efficiency was determined by gene expression analysis with QPCR (see Supplementary information).

Retinal whole mounts

Mice were sacrificed on postnatal day 28 [36]. Mouse eyes were collected and fixed in 4% paraformaldehyde (PFA). Retinas were dissected, fixed in 4% PFA, dehydrated and stored in methanol at −20°C. Before analysis, retinal whole-mounts were rehydrated, permeabilized in PBS, 1% BSA, 0.5% Triton X-100 and washed with PBS. Retinal whole-mounts were blocked in PBlec (PBS, pH 6.8, 1% Triton X-100, 0.1 mM $CaCl_2$, 0.1 mM $MgCl_2$, 0.1 mM $MnCl_2$), and incubated in Alexa 488-labeled isolectin B4 (Sigma-Aldrich) in PBlec. After extensive washing in PBS, the retinas were flat mounted in Vectashield (Vector Laboratories, Burlingame, CA). Images were taken using a wide-field fluorescence microscope (Leica) or confocal microscope (Leica). For vascular quantification, the total number of branch points in the superficial, intermediate and outer plexus was counted per microscopic field [36], or the number of radial veins and arteries in the superficial plexus was counted per retina (see Supplementary information).

Aortic ring assay

After sacrificing the mice, thoracic aortae were dissected, adipose tissue/fat removed, washed and cut into 1-mm rings [37]. Next, the aortic rings were embedded in Matrigel (growth factor reduced, BD Biosciences, Oxford, United Kingdom) and cultured in M199 medium (Invitrogen) containing 2% FCS, 12% ECGS (Sigma-Aldrich), 200μl/ml gentamycin (Invitrogen), 2.5 μl/ml Amphotericin (Lonza) in the presence or absence of LT (30ng/ml), LIGHT (30 ng/ml), TNF (100 ng/ml) or VEGF (100 ng/ml) (all R&D Systems). After 8 days, microvessel outgrowth was analyzed using Leica imaging software.

Antigen Induced Arthritis

Antigen-induced arthritis was performed previously [38]. In brief, Wt (n=5) and $Nik^{-/-}$ (n=5) mice were immunized with 100 μg methylated (m)BSA (Sigma-Aldrich) emulsified in 0.1 ml complete Freund's adjuvant (BD) intradermally at the base of the tail. Simultaneously, 1 μg pertussis toxin (List Biological Laboratories Inc., Campbell, CA) was injected intraperitoneally as an additional adjuvant. Arthritis was induced at day 21 by intra-articular injection of 100 μg of mBSA into the right knee joint, while the left knee joint was injected with PBS alone. Mice were sacrificed on day 32. For histological grading of the arthritis, hind paws were dissected and fixed in 10% buffered formalin. Fixed tissues were decalcified in EDTA, dehydrated, and embedded in paraffin. Sagittal sections (5 μm) were stained with H&E, anti-CD31 (sc-1505, Santa Cruz Biotechnology), or anti-CXCL12 (MAB350, R&D Systems). Next, slides were incubated with secondary antibody rabbit-anti-goat (sc-2922, Santa Cruz Biotechnology) or goat anti-mouse (P044701, DAKO), and streptavidin labeled with horseradish peroxidase. Biotinylated tyramine was used for amplification. Slides were scored blindly by 2 independent researchers. Inflammation was scored semiquantitatively on a scale of 0 to 4, and synovial blood vessels were counted.

B16 melanoma bone metastasis model

The melanoma bone metastasis model was performed previously [39]. In brief, Wt mice (n=6) and $Nik^{-/-}$ mice (n=6) at 38–46 days of age were anesthetized and inoculated intra-arterially with 10^5 B16-FL murine melanoma cells in 50 μl of PBS. Mice were sacrificed on day 12 after tumor cell injection. For histological analysis, hind paws were dissected and fixed in 10% buffered formalin. Fixed tissues were decalcified in EDTA, dehydrated, and embedded in paraffin. Sagittal sections (5 μm) were stained with H&E, anti-CD31 (sc-1505, Santa Cruz Biotechnology) or anti-CXCL12 (MAB350, R&D Systems). Next, slides were incubated with secondary antibody rabbit-anti-goat (sc-2922, Santa Cruz Biotechnology) or goat anti-mouse (P044701, DAKO), and streptavidin labeled with horseradish peroxidase. Biotinylated tyramine was used for amplification. Tumor blood vessels were counted by 2 independent researchers.

Statistical analysis

All data are presented as mean ± standard error of the mean (SEM). Statistical analysis was carried out using Prism Software (GraphPad). For statistical comparison, mean values per group were compared by unpaired Mann-Whitney U test. P-values <0.05 were considered statistically significant (*P<0.05, **P<0.01).

RESULTS

NIK is highly expressed in endothelial cells of inflamed RA synovial tissue

The non-canonical NF-κB stimuli CD40L, LT and LIGHT are highly expressed in RA synovial tissue [24-26]. Therefore, we investigated whether the non-canonical NF-κB pathway is activated in RA synovial tissue by studying the expression and distribution of NIK using immunohistochemistry (IHC). Interestingly, NIK was mainly expressed by vascular structures, both in early and in established RA (Fig. 1A,B), whereas normal healthy synovial tissue did not contain NIK-positive vessels (Fig. S1A). Subsequent double-immunofluorescence microscopy analysis revealed that NIK strongly co-localized with the EC marker CD31/34 in small blood vessels (Fig. 1D). Quantification of each NIK^+ and $CD31/34^+$ area in double-stained tissue sections showed that approximately three-quarters (74.4 ± 5.5%; n=10) of EC in RA synovial tissue were NIK-positive. These results fuel the hypothesis that NIK may be of importance in either activation of EC or inflammation-induced neovascularization.

Functional non-canonical NF-κB signaling in RA synovial tissue endothelial cells

Non-canonical NF-κB signaling in EC induces the pro-angiogenic chemokine CXCL12 that also mediates lymphocyte transendothelial migration [16,17]. To investigate whether non-canonical NF-κB signaling is functional in NIK-expressing EC in RA synovial tissue, we performed additional stainings for T-loop activated phospho-IKKα, the non-canonical NF-κB subunit p52 and CXCL12. NIK expression (Fig 1) colocalized with T-loop activated phospho-IKKα (Fig. 1E), strongly suggesting that the non-canonical NF-κB pathway is activated in synovial EC. In addition, both p52 (Fig. S1B) and CXCL12 (Fig. S1C) were expressed in blood vessels, further strengthening that the non-canonical NF-κB pathway is

functionally active in EC in RA synovial tissue. The NF-κB subunit RelB was also expressed in RA synovial tissue, but not exclusively in EC (Fig. S1D), which is in line with previous reports [40].

NIK is also expressed by endothelial cells in tumor tissues

The non-canonical NF-κB pathway has been demonstrated to play an important role in tumor development [28,29,41]. However, these studies did not focus on EC or angiogenesis. To investigate whether NIK expression in newly formed blood vessels is specific for RA synovial tissue or also occurs in tumor neovascularization, we evaluated NIK expression in human melanoma, renal cell carcinoma, breast cancer, colorectal cancer, and pancreatic cancer. In these tissues we detected NIK in vascular structures as well (Fig. 2A-E). Double-immunofluorescence microscopy demonstrated that NIK and T-loop activated phospho-IKKα were highly expressed by essentially all blood vessel EC in cancer tissues, as depicted for breast cancer (Fig. 2F,G). Since both inflammation-induced angiogenesis and tumor-associated angiogenesis are in many aspects different from normal angiogenesis [1], we also studied the expression of NIK in blood vessels of healthy human tissues. Interestingly, EC in blood vessels of normal human skin (Fig. 2H) and other normal healthy tissues did not exhibit NIK expression (Fig. S2). Collectively, these data show that both in chronic (synovial) inflammation and in tumors, NIK expression is exclusively vascular and increased selectively during neovascular growth.

Non-canonical NF-κB signaling induces in vitro sprouting of endothelial cells

Next, we evaluated the role of the non-canonical NF-κB pathway in vitro. HMVEC were seeded on fibrin matrices in the presence of bFGF/TNFα to facilitate outgrowth of tube-like structures, as a model for pathological sprout formation [14]. A significantly increased tube formation was observed when LT, LIGHT or CD40L was added to bFGF/TNFα (Fig. 3A,B). This pro-angiogenic effect of the non-canonical NF-κB stimuli was dose-dependent as shown for LT (Fig. S3A). To investigate whether the enhanced tube formation was dependent on canonical or non-canonical NF-κB signaling, we used siRNAs specifically targeting IKKβ, the essential kinase in canonical NF-κB signaling, or NIK or IKKα, the main kinases of the non-canonical NF-κB pathway (siIKKβ, siNIK or siIKKα). QPCR analysis demonstrated that target genes were all specifically knocked down 80-90% by the corresponding siRNAs (Fig. S3B-D). Additional protein data confirmed that gene knock-down of NIK also prevented p100/p52 processing as assessed by western blot (Fig. S3E). Specific siRNA-mediated gene silencing of NIK or IKKα blocked LT, LIGHT and CD40L-enhanced tube formation significantly (Fig. 3C-F). In contrast, siIKKβ blocked tube formation only partially. Furthermore, we also observed an effect of siNIK and siIKKα on basal tube formation, suggesting that the non-canonical pathway also contributed to basal sprouting in this model, although to a lesser extent. Altogether, it can be concluded that LT, LIGHT and CD40L-induced tube formation relies mostly on non-canonical NF-κB signaling, a hitherto unknown function of this pathway in EC. We confirmed that non-canonical NF-κB signaling in HMVECs results in nuclear translocation of p52 and DNA-binding activity, which significantly decreased in siNIK treated cells (Fig. S3F). To further unravel the underlying mechanisms of NIK-induced angiogenesis in EC we performed PCR arrays of angiogenesis related genes. Interestingly, knock-down of NIK in EC resulted in

significantly reduced expression levels of ANGPT2, BTG1, CD55, CSF3, CXCL4, CXCL5, CXCL6, CXCL9, CXCL11, CXCL12, FGF13, FN1, IFNB1, IL-6, IL-8, KITLG, PDGFB, PDGF, PGF, STAB1, and *TGFA* after LIGHT stimulation (Table S1).

Normal developmental angiogenesis, but reduced pathological angiogenic responses after genetic deletion of NIK

We made use of $Nik^{-/-}$ mice to further investigate the importance of NIK in angiogenesis in vivo. $Nik^{-/-}$ mice lack peripheral lymph nodes and have altered T and B cell responses [32]. Despite these defects, $Nik^{-/-}$ mice are viable and appear to have a normal vasculature, suggesting that developmental angiogenesis is not impaired. To confirm this, we studied the vascular network in the retina of $Nik^{-/-}$ mice compared to Wt mice on postnatal day 28, when all three vascular layers are fully mature [36]. No differences were detected in the number of branch points in the superficial, intermediate and outer plexus between $Nik^{-/-}$ and Wt mice (Fig. 4A,B). Also, no abnormalities in the mean number of arteries and veins were observed (Fig. S4). To further study the importance of non-canonical NF-κB signaling in angiogenesis, we tested the angiogenic potential of Wt and $Nik^{-/-}$ mice in the aortic ring assay. Aortic rings from Wt and $Nik^{-/-}$ mice exhibited normal microvessel outgrowth after VEGF and TNFα stimulation, indicating that both VEGF- and TNFα-induced (canonical NF-κB dependent) angiogenesis are unaffected (Fig. 4C,D), which is in line with the normal developmental angiogenesis of these mice. In contrast, whereas the non-canonical NF-κB stimuli LT and LIGHT significantly induced microvessel outgrowth in Wt mice, no microvessel outgrowth was observed in $Nik^{-/-}$ mice after LT or LIGHT stimulation (Fig. 4E,F). This strongly suggests that angiogenesis under pathological conditions, in the presence of stimuli such as LT and LIGHT, is dependent on NIK and subsequent non-canonical NF-κB signaling.

$Nik^{-/-}$ mice exhibit reduced inflammation-induced and tumor-associated angiogenesis

Finally, we investigated whether pathological angiogenesis is dependent on non-canonical NF-κB signaling *in vivo*. To study inflammation-induced angiogenesis, we made use of an experimental arthritis model. Previously, we reported that NIK is important in the immune and bone-destructive components of inflammatory arthritis in antigen-induced arthritis [38]. Histology of the arthritic hind paws of $Nik^{-/-}$ mice revealed less synovial inflammation (Fig. 5A). Quantification of the total number of synovial blood vessels demonstrated a 50% reduction in $Nik^{-/-}$ mice compared to Wt mice (Wt 20.00 ± 5.07 vs. $Nik^{-/-}$ 10.20 ± 3.02; P=0.1354) (Fig. 5B). In addition, we found that the number of $CXCL12^{+}$ blood vessels was significantly decreased in the synovial tissue of $Nik^{-/-}$ mice (Wt 26.60 ± 1.63 vs $Nik^{-/-}$ 13.00 ± 1.23; P=0.007)(Fig. 5C). This was accompanied by significantly reduced inflammation scores (Wt 3.40 ± 0.20 vs. $Nik^{-/-}$ 1.67 ± 0.33; P=0.008)(Fig. 5D). These findings suggest that non-canonical NF-κB signaling contributes to pathological, inflammation-induced angiogenesis.

Next, we investigated the contribution of NIK to tumor-associated angiogenesis using the B16 melanoma model. In this model we have previously established that genetic deletion of NIK blocks tumor-induced loss of trabecular bone [39]. Here, we demonstrate that $Nik^{-/-}$ mice have a significantly reduced total number of blood vessels inside the tumor compared

to wild type mice (Wt 8,33 ± 6,36 vs. $Nik^{-/-}$ 0,50 ± 0,34; P=0.05) (Fig. 5E, F). In addition, the number of $CXCL12^{+}$ blood vessels was significantly decreased in the tumor tissue of $Nik^{-/-}$ mice (Wt 12.5 ± 1.29 vs $Nik^{-/-}$ 2.33 ± 0.33; P=0.005)(Fig. 5G), underlining the important role of non-canonical NF-κB signaling in pathological angiogenesis.

DISCUSSION

Our data provide compelling evidence that NIK and subsequent non-canonical NF-κB signaling regulate inflammation-induced and tumor-associated angiogenesis, whereas NIK is dispensable for angiogenesis during development. Therefore, we propose that non-canonical NF-κB signaling specifically regulates pathological angiogenesis.

The non-canonical NF-κB pathway has been demonstrated to play an important role in tumor development [28,29,41]. However, these studies mainly focused on the intrinsic role of non-canonical NF-κB signaling in tumor cells. Our study shows for the first time that NIK is expressed and active in EC in inflamed RA synovial tissue as well as in a variety of tumor tissues, whereas the vasculature in normal healthy tissues does not express NIK. Importantly, our findings also identify NIK as a potential new therapeutic target in chronic inflammatory diseases, in particular arthritis, and cancer, since targeting components of the non-canonical NF-κB pathway efficiently blocked angiogenic responses. Previously, IKKβ-mediated canonical NF-κB signaling has been implicated in angiogenesis [42]. However, knock-down of NIK or IKKα abrogated tube formation far more effectively than knock-down of IKKβ in our sprouting assay. Therefore, we conclude that LT, LIGHT and CD40L-induced tube formation relies mostly on non-canonical NF-κB signaling, a hitherto unknown function of this pathway in EC. Interestingly, knock-down of NIK or IKKα also blocked tube formation under basal conditions in the presence of low amounts of TNF and bFGF. This suggests that the non-canonical pathway is already somewhat activated in EC in these conditions. A likely explanation for this is that EC express both CD40 and CD40L [43], which could induce non-canonical NF-κB signaling in EC due to cell-cell contact of adjacent EC. The angiogenesis PCR array data point towards a pleiotropic role of non-canonical NF-κB signaling in chemokine expression and several other pro-angiogenic pathways in EC, as subsequent gene ontology analysis did not reveal involvement of one specific established angiogenesis pathway.

Our studies in $Nik^{-/-}$ mice demonstrate that both developmental retinal angiogenesis and VEGF-induced or TNFα-induced angiogenic responses are unaffected. In contrast, we observed significantly reduced non-canonical NF-κB-dependent microvessel outgrowth in the aortic ring assay, and clearly impaired pathological, inflammation-induced angiogenesis in the antigen-induced arthritis model in $Nik^{-/-}$ mice. Of note, the observed reduction in arthritis and histological inflammation scores in $Nik^{-/-}$ mice may at least in part be due to impaired angiogenesis, since the number of $CXCL12^{+}$ blood vessels was significantly reduced in $Nik^{-/-}$ mice.

Genetic ablation of NIK resulted in an almost complete block in pathological, tumor-associated angiogenesis in the B16 melanoma model. Scattered evidence from the literature underscores our findings that one of the signaling pathways of importance in tumor

neoangiogenesis, and possibly also in anti-VEGF treatment resistance, may be the non-canonical NF-κB signaling pathway. Colorectal cancer EC have been demonstrated to exhibit significantly increased IKKα expression compared to EC in adjacent normal tissue [30]. Furthermore, in EC expression of CXCL12, a chemokine that plays an important role in angiogenesis and the homing of CXCR4 expressing endothelial progenitor cells (EPC) [16], is regulated by non-canonical NF-κB signaling [17]. EPC have been demonstrated to contribute to pathological angiogenesis both in developing tumors [44] and in lethal macrometastasis [45], as well as in the inflamed RA synovium [46,47]. Therefore, non-canonical NF-κB-induced CXCL12 in cancer EC [19] and synovial tissue EC [18] may serve as a focal point modulating vasculogenesis, angiogenesis, and the attraction of immune cells.

Current strategies aimed at inhibition of angiogenesis in patients affect both pathological and physiological angiogenesis, resulting in unwanted side-effects. We hypothesize that targeting of NIK and subsequent non-canonical NF-κB signaling in EC may overcome this problem. In addition, targeting of NIK could be combined with current anti-angiogenic cancer treatments to prevent or rescue resistance. In RA, pathological angiogenesis drives chronic inflammation and therefore also is an attractive therapeutic target [46]. The recent description of the crystal structure of NIK may facilitate the development of new potent inhibitors [48,49]. These inhibitors could be directed specifically to EC using a multimodular recombinant protein that specifically binds to cytokine-activated endothelium, which has been demonstrated to work very elegantly under inflammatory conditions *in vivo* [50].

Taken together our studies point towards an important role of the non-canonical NF-κB pathway in pathological angiogenesis. Therefore, selective inhibition of non-canonical NF-κB signaling in EC could be used as a novel therapeutic strategy, which may not only be beneficial in chronic inflammatory diseases such as RA and cancer, but potentially also other diseases characterized by aberrant neovascularization, like ocular diseases and atherosclerosis.

Supplementary Material

Refer to Web version on PubMed Central for supplementary material.

Acknowledgments

We thank the arthroscopy team of our for obtaining the synovial tissue biopsies, Prof. dr. Sandrine Florquin for providing tumor and healthy tissue specimens, Dr. Marcel Teunissen for providing normal human skin biopsies, and Dr. Rosalie Luiten and Esther Tjin for melanoma samples. We also acknowledge the invaluable technical support of Linda Hartkamp and Boy Helder, as well as the expert technical support of Dr. Corine van der Horst with respect to digital imaging analysis. We thank Prof. dr. Victor van Hinsbergh for critically reading the manuscript. This work was supported by a Veni grant of the Netherlands Organisation for Scientific Research (NWO) and a Clinical Fellowship (ZonMw) to S.W. Tas, and the National Institutes of Health (NIH) to D.V. Novack (grant number AR052705). P. Koolwijk received a grant of the Netherlands Initiative for Regenerative Medicine (NIRM).

This work was supported by a Veni grant of the Netherlands Organisation for Scientific Research (NWO) and a Clinical Fellowship (ZonMw) to S.W. Tas, and the National Institutes of Health (NIH) to D.V. Novack (grant number AR052705). P. Koolwijk received a grant of the Netherlands Initiative for Regenerative Medicine (NIRM).

REFERENCES

1. Carmeliet P. Angiogenesis in life, disease and medicine. Nature. 2005; 438:932–936. [PubMed: 16355210]
2. Ferrara N. VEGF and the quest for tumour angiogenesis factors. Nat Rev Cancer. 2002; 2:795–803. [PubMed: 12360282]
3. Kim KJ, Li B, Winer J, et al. Inhibition of vascular endothelial growth factor-induced angiogenesis suppresses tumour growth in vivo. Nature. 1993; 362:841–844. [PubMed: 7683111]
4. Fava RA, Olsen NJ, Spencer-Green G, et al. Vascular permeability factor/endothelial growth factor (VPF/VEGF): accumulation and expression in human synovial fluids and rheumatoid synovial tissue. The Journal of experimental medicine. 1994; 180:341–346. [PubMed: 8006592]
5. Choi ST, Kim JH, Seok JY, et al. Therapeutic effect of anti-vascular endothelial growth factor receptor I antibody in the established collagen-induced arthritis mouse model. Clinical rheumatology. 2009; 28:333–337. [PubMed: 19101756]
6. Sone H, Kawakami Y, Sakauchi M, et al. Neutralization of vascular endothelial growth factor prevents collagen-induced arthritis and ameliorates established disease in mice 6. BiochemBiophysResCommun. 2001; 281:562–568.
7. Ellis LM, Hicklin DJ. VEGF-targeted therapy: mechanisms of anti-tumour activity. Nature reviews Cancer. 2008; 8:579–591.
8. Welti J, Loges S, Dimmeler S, et al. Recent molecular discoveries in angiogenesis and antiangiogenic therapies in cancer. The Journal of clinical investigation. 2013; 123:3190–3200. [PubMed: 23908119]
9. Bakall B, Folk JC, Boldt HC, et al. Aflibercept therapy for exudative age-related macular degeneration resistant to bevacizumab and ranibizumab. American journal of ophthalmology. 2013; 156:15–22. [PubMed: 23706500]
10. Oeckinghaus A, Hayden MS, Ghosh S. Crosstalk in NF-kappaB signaling pathways. Nature immunology. 2011; 12:695–708. [PubMed: 21772278]
11. Senftleben U, Cao Y, Xiao G, et al. Activation by IKKalpha of a second, evolutionary conserved, NF-kappa B signaling pathway. Science. 2001; 293:1495–1499. [PubMed: 11520989]
12. Tas SW, Vervoordeldonk MJ, Tak PP. Gene therapy targeting nuclear factor-kappaB: towards clinical application in inflammatory diseases and cancer. CurrGene Ther. 2009; 9:160–170.
13. De Martin MR, Hoeth M, Hofer-Warbinek R, et al. The transcription factor NF-kappa B and the regulation of vascular cell function. ArteriosclerThrombVascBiol. 2000; 20:E83–E88.
14. Koolwijk P, van Erck MG, de Vree WJ, et al. Cooperative effect of TNFalpha, bFGF, and VEGF on the formation of tubular structures of human microvascular endothelial cells in a fibrin matrix. Role of urokinase activity 1. JCell Biol. 1996; 132:1177–1188. [PubMed: 8601593]
15. Huang S, Robinson JB, Deguzman A, et al. Blockade of nuclear factor-kappaB signaling inhibits angiogenesis and tumorigenicity of human ovarian cancer cells by suppressing expression of vascular endothelial growth factor and interleukin 8. Cancer Res. 2000; 60:5334–5339. [PubMed: 11034066]
16. Petit I, Jin D, Rafii S. The SDF-1-CXCR4 signaling pathway: a molecular hub modulating neo-angiogenesis. Trends Immunol. 2007; 28:299–307. [PubMed: 17560169]
17. Madge LA, Kluger MS, Orange JS, et al. Lymphotoxin-alpha 1 beta 2 and LIGHT induce classical and noncanonical NF-kappa B-dependent proinflammatory gene expression in vascular endothelial cells. JImmunol. 2008; 180:3467–3477. [PubMed: 18292573]
18. Santiago B, Baleux F, Palao G, et al. CXCL12 is displayed by rheumatoid endothelial cells through its basic amino-terminal motif on heparan sulfate proteoglycans. Arthritis research & therapy. 2006; 8:R43. [PubMed: 16507142]
19. Teicher BA, Fricker SP. CXCL12 (SDF-1)/CXCR4 pathway in cancer. Clinical cancer research : an official journal of the American Association for Cancer Research. 2010; 16:2927–2931. [PubMed: 20484021]
20. Drayton DL, Bonizzi G, Ying X, et al. I kappa B kinase complex alpha kinase activity controls chemokine and high endothelial venule gene expression in lymph nodes and nasal-associated lymphoid tissue. JImmunol. 2004; 173:6161–6168. [PubMed: 15528353]

21. Browning JL, Allaire N, Ngam-Ek A, et al. Lymphotoxin-beta receptor signaling is required for the homeostatic control of HEV differentiation and function. Immunity. 2005; 23:539–550. [PubMed: 16286021]
22. Manzo A, Paoletti S, Carulli M, et al. Systematic microanatomical analysis of CXCL13 and CCL21 in situ production and progressive lymphoid organization in rheumatoid synovitis. EurJImmunol. 2005; 35:1347–1359.
23. Schrama D, thor SP, Fischer WH, et al. Targeting of lymphotoxin-alpha to the tumor elicits an efficient immune response associated with induction of peripheral lymphoid-like tissue. Immunity. 2001; 14:111–121. [PubMed: 11239444]
24. Takemura S, Braun A, Crowson C, et al. Lymphoid neogenesis in rheumatoid synovitis 4. JImmunol. 2001; 167:1072–1080. [PubMed: 11441118]
25. Pierer M, Brentano F, Rethage J, et al. The TNF superfamily member LIGHT contributes to survival and activation of synovial fibroblasts in rheumatoid arthritis 1. Rheumatology(Oxford). 2007; 46:1063–1070. [PubMed: 17426140]
26. Kang YM, Zhang X, Wagner UG, et al. CD8 T cells are required for the formation of ectopic germinal centers in rheumatoid synovitis. JExpMed. 2002; 195:1325–1336.
27. Hehlgans T, Stoelcker B, Stopfer P, et al. Lymphotoxin-beta receptor immune interaction promotes tumor growth by inducing angiogenesis 5. Cancer Res. 2002; 62:4034–4040. [PubMed: 12124338]
28. Daller B, Musch W, Rohrl J, et al. Lymphotoxin-beta receptor activation by lymphotoxin-alpha(1)beta(2) and LIGHT promotes tumor growth in an NFkappaB-dependent manner 1. IntJCancer. 2011; 128:1363–1370.
29. Wolf MJ, Seleznik GM, Zeller N, et al. The unexpected role of lymphotoxin beta receptor signaling in carcinogenesis: from lymphoid tissue formation to liver and prostate cancer development 1. Oncogene. 2010; 29:5006–5018. [PubMed: 20603617]
30. Charalambous MP, Lightfoot T, Speirs V, et al. Expression of COX-2, NF-kappaB-p65, NF-kappaB-p50 and IKKalpha in malignant and adjacent normal human colorectal tissue. BrJCancer. 2009; 101:106–115.
31. de Hair MJ, Harty LC, Gerlag DM, et al. Synovial tissue analysis for the discovery of diagnostic and prognostic biomarkers in patients with early arthritis. The Journal of rheumatology. 2011; 38:2068–2072. [PubMed: 21885519]
32. Yin L, Wu L, Wesche H, et al. Defective lymphotoxin-beta receptor-induced NF-kappaB transcriptional activity in NIK-deficient mice. Science. 2001; 291:2162–2165. [PubMed: 11251123]
33. Smeets TJ, Barg EC, Kraan MC, et al. Analysis of the cell infiltrate and expression of proinflammatory cytokines and matrix metalloproteinases in arthroscopic synovial biopsies: comparison with synovial samples from patients with end stage, destructive rheumatoid arthritis. AnnRheumDis. 2003; 62:635–638.
34. van Hinsbergh VW, Sprengers ED, Kooistra T. Effect of thrombin on the production of plasminogen activators and PA inhibitor-1 by human foreskin microvascular endothelial cells. ThrombHaemost. 1987; 57:148–153.
35. van Hensbergen Y, Broxterman HJ, Peters E, et al. Aminopeptidase inhibitor bestatin stimulates microvascular endothelial cell invasion in a fibrin matrix. Thrombosis and haemostasis. 2003; 90:921–929. [PubMed: 14597989]
36. Stahl A, Connor KM, Sapieha P, et al. The mouse retina as an angiogenesis model. Investigative ophthalmology & visual science. 2010; 51:2813–2826. [PubMed: 20484600]
37. Baker M, Robinson SD, Lechertier T, et al. Use of the mouse aortic ring assay to study angiogenesis 1. NatProtoc. 2012; 7:89–104.
38. Aya K, Alhawagri M, Hagen-Stapleton A, et al. NF-(kappa)B-inducing kinase controls lymphocyte and osteoclast activities in inflammatory arthritis. JClinInvest. 2005; 115:1848–1854.
39. Vaira S, Johnson T, Hirbe AC, et al. RelB is the NF-kappaB subunit downstream of NIK responsible for osteoclast differentiation. ProcNatlAcadSciUSA. 2008; 105:3897–3902.
40. Pettit AR, MacDonald KP, O'Sullivan B, et al. Differentiated dendritic cells expressing nuclear RelB are predominantly located in rheumatoid synovial tissue perivascular mononuclear cell aggregates. Arthritis Rheum. 2000; 43:791–800. [PubMed: 10765923]

41. Keats JJ, Fonseca R, Chesi M, et al. Promiscuous mutations activate the noncanonical NF-kappaB pathway in multiple myeloma. Cancer Cell. 2007; 12:131–144. [PubMed: 17692805]
42. Yu HG, Yu LL, Yang Y, et al. Increased expression of RelA/nuclear factor-kappa B protein correlates with colorectal tumorigenesis. Oncology. 2003; 65:37–45. [PubMed: 12837981]
43. Mach F, Schonbeck U, Sukhova GK, et al. Functional CD40 ligand is expressed on human vascular endothelial cells, smooth muscle cells, and macrophages: implications for CD40-CD40 ligand signaling in atherosclerosis. Proceedings of the National Academy of Sciences of the United States of America. 1997; 94:1931–1936. [PubMed: 9050882]
44. Lyden D, Hattori K, Dias S, et al. Impaired recruitment of bone-marrow-derived endothelial and hematopoietic precursor cells blocks tumor angiogenesis and growth. NatMed. 2001; 7:1194–1201.
45. Gao D, Nolan DJ, Mellick AS, et al. Endothelial progenitor cells control the angiogenic switch in mouse lung metastasis. Science. 2008; 319:195–198. [PubMed: 18187653]
46. Szekanecz Z, Besenyei T, Szentpetery A, et al. Angiogenesis and vasculogenesis in rheumatoid arthritis. CurrOpinRheumatol. 2010; 22:299–306.
47. Distler JH, Beyer C, Schett G, et al. Endothelial progenitor cells: novel players in the pathogenesis of rheumatic diseases. Arthritis Rheum. 2009; 60:3168–3179. [PubMed: 19877034]
48. de Leon-Boenig G, Bowman KK, Feng JA, et al. The Crystal Structure of the Catalytic Domain of the NF-kappaB Inducing Kinase Reveals a Narrow but Flexible Active Site. Structure. 2012; 20:1704–1714. [PubMed: 22921830]
49. Li K, McGee LR, Fisher B, et al. Inhibiting NF-kappaB-inducing kinase (NIK): discovery, structure-based design, synthesis, structure-activity relationship, and co-crystal structures. Bioorganic & medicinal chemistry letters. 2013; 23:1238–1244. [PubMed: 23374866]
50. Sehnert B, Burkhardt H, Wessels JT, et al. NF-kappaB inhibitor targeted to activated endothelium demonstrates a critical role of endothelial NF-kappaB in immune-mediated diseases. Proceedings of the National Academy of Sciences of the United States of America. 2013; 110:16556–16561. [PubMed: 24062461]

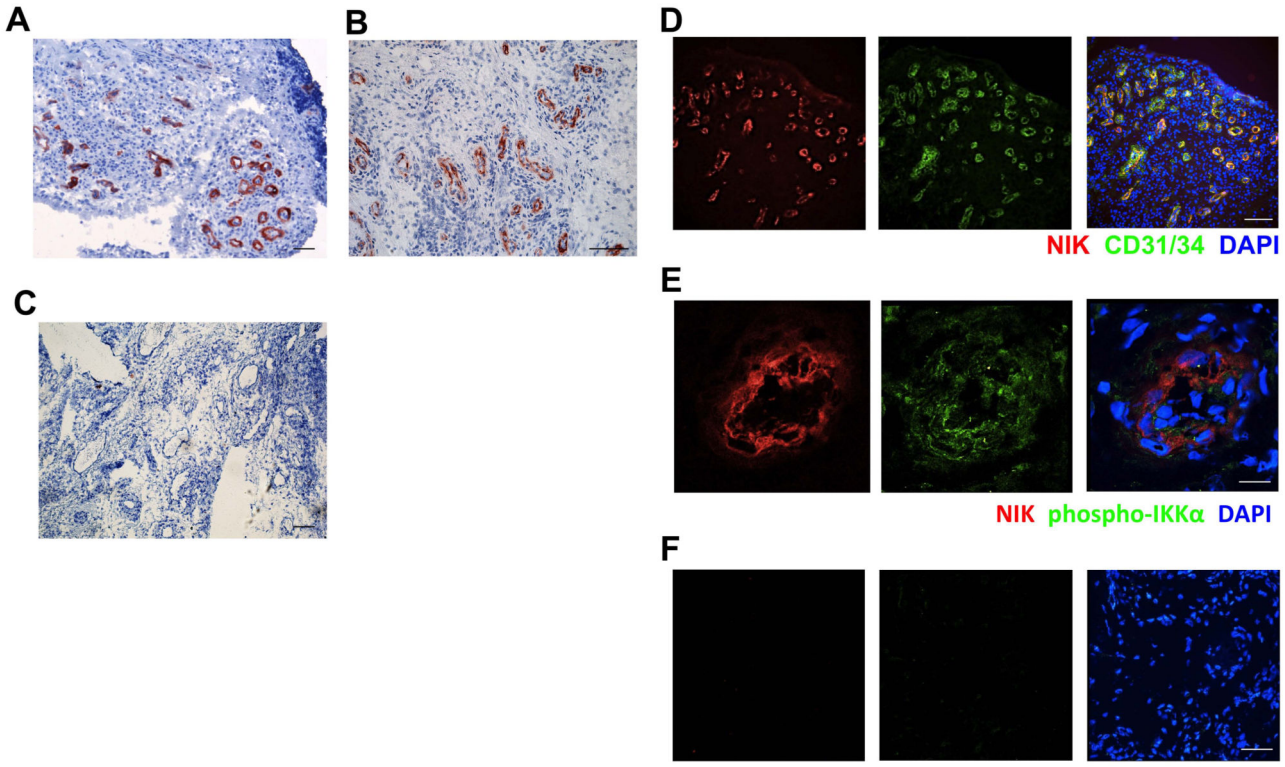

Figure 1. NIK expression in synovial tissue endothelial cells of rheumatoid arthritis patients

Synovial tissue sections from early and established RA patients showing **A,B** IHC staining of NIK and **C**, the isotype control (scale bar A,C 100 μm, scale bar B 200 μm). **D,** IF staining of NIK (red), CD31/34 (green) and nuclei (blue) (scale bar, 100 μm). **E**. IF staining of NIK (red), phospho-IKKα (green) and nuclei (blue) (scale bar 12.4 μm), and **F** isotype control of E (scale bar 27.9 μm). Representative pictures are shown (n=10 different RA synovial tissues/staining).

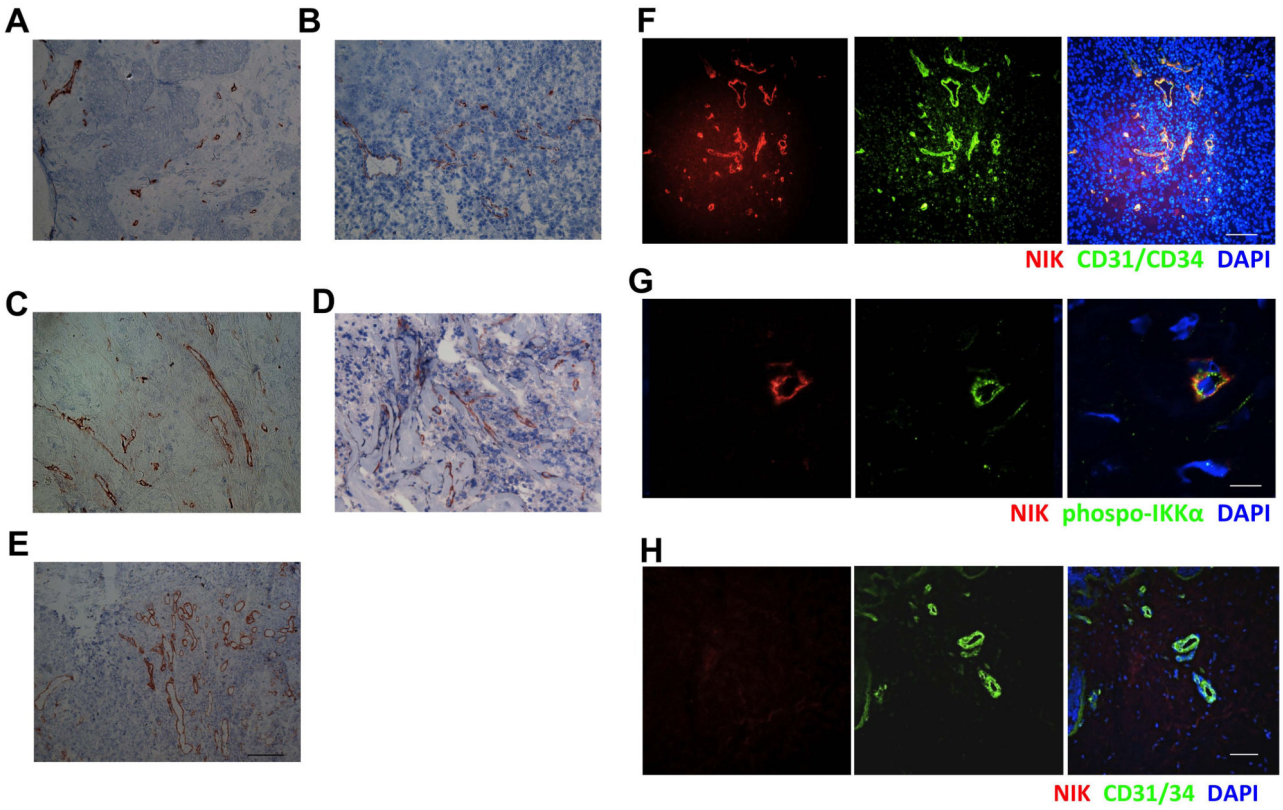

Figure 2. NIK is expressed in endothelial cells in tumor tissues

NIK expression in **A**, renal carcinoma tissue **B**, breast cancer tissue **C,** pancreatic cancer tissue **D**, melanoma tissue **E,** colorectal cancer tissue and **F,** IF staining on NIK (red) and CD31/CD34 (green) and nuclei (blue), in breast cancer tissue. **G,** IF staining on NIK (red) and phospho-IKKα (green) and nuclei (blue) in breast cancer tissue. **H,** IF on NIK (red) and CD31/CD34 (green) and nuclei (blue) in normal skin. Representative pictures are shown (n=5-6 patients or healthy donors, 2 independent experiments) (scale bars A-F, H, 100 μm; scale bar G 11.2 μm).

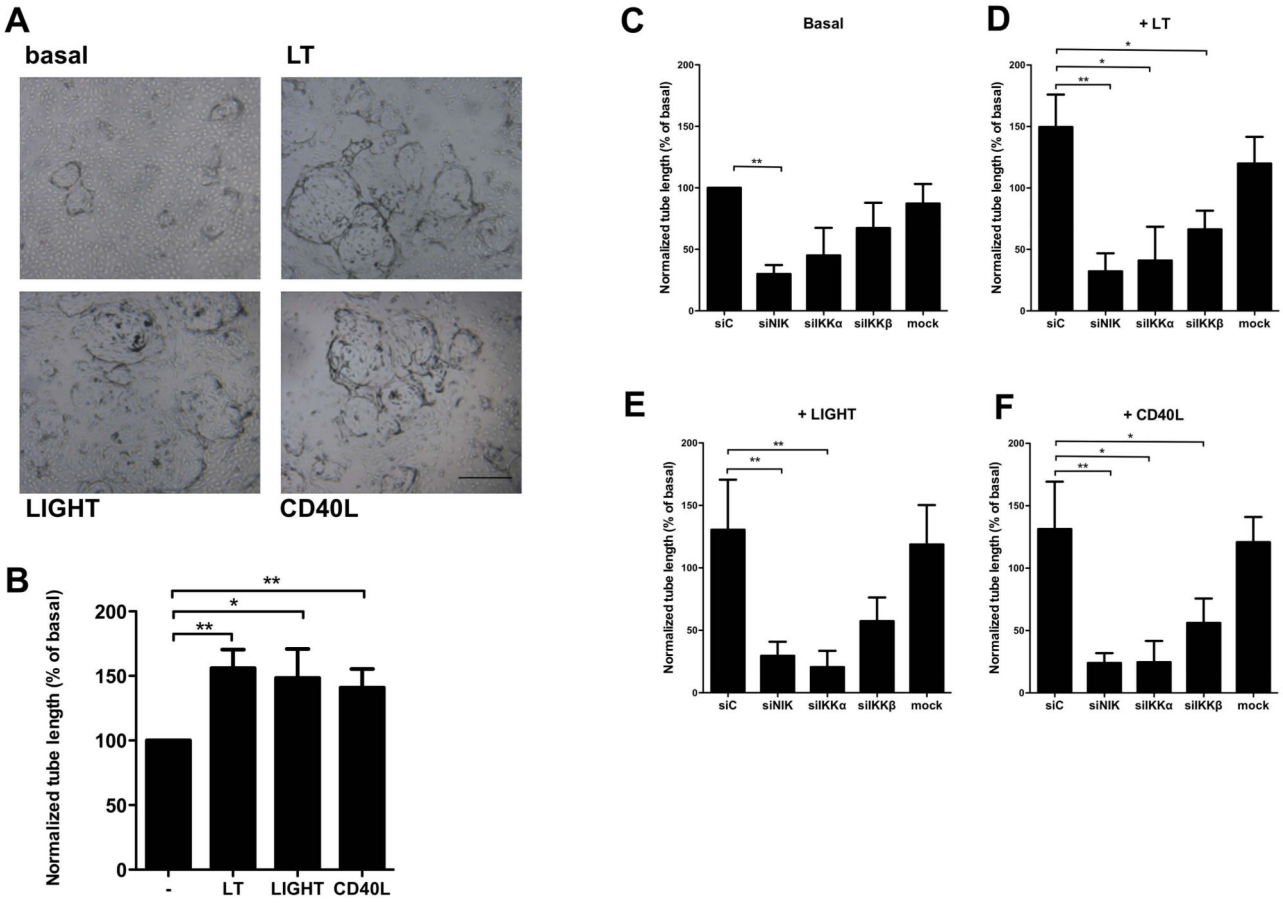

Figure 3. Non-canonical NF-κB signaling induces in vitro sprouting of endothelial cells

A, Representative pictures of tube formation by HMVEC under basal conditions or after LT-, LIGHT- and CD40L- stimulation (scale bar all panels, 500 μm). **B,** Quantification of LT-, LIGHT- and CD40L-enhanced tube formation. n=7 per group, 3 independent experiments. **C-F,** HMVEC were transfected by the indicated siRNAs. Scrambled non-targeting siRNA (= siC) was used as a control. **C,** Basal tube formation. **D,** LT-enhanced tube formation. **E,** LIGHT-enhanced tube formation. **F,** CD40L-enhanced tube formation. n=6 per group, 3 independent experiments. All panels mean±SEM: *P<0.05 **P<0.01 Specific knockdown of the genes targeted by the siRNAs is shown in suppl. figure 4.

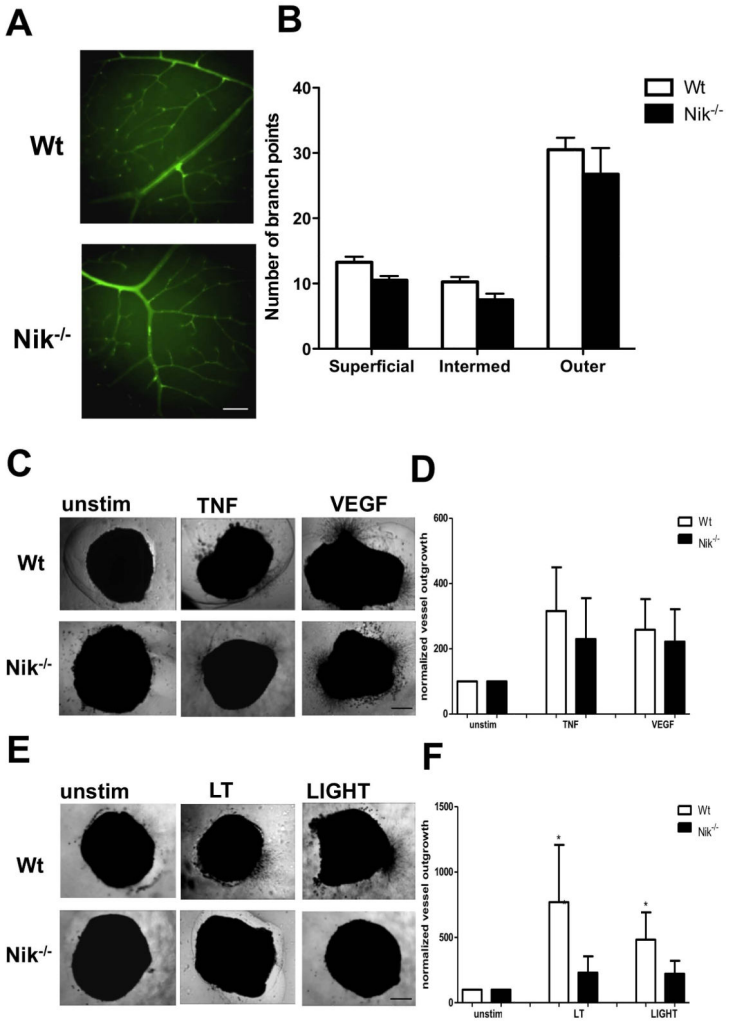

Figure 4. Genetic deletion of NIK results in reduced pathological angiogenic responses

A, Representative retinas from Wt and Nik$^{-/}$ mice, stained with isolectin B4 (green) (scale bar for both panels, 100 μm). **B,** Quantification of vessel branching in the superficial, intermediate and outer vascular plexus. **C,** Aortic rings of Wt and Nik$^{-/-}$ mice cultured in medium alone, TNF-α or VEGF. Representative pictures are shown (scale bar all panels, 500 μm). **D,** Quantification of TNF-α and VEGF-induced aortic vessel outgrowth. **E,** Representative pictures of unstimulated, LT- or LIGHT-stimulated aortic rings (scale bar all panels, 500 μm). **F,** Quantification of LT- and LIGHT-induced aortic vessel outgrowth. Panels B,C,D n=4 per group, 2 independent experiments. Panels A,E,F n=5 per group, 2 independent experiments. Panels B,D,F, represent mean±SEM *<P0.05.

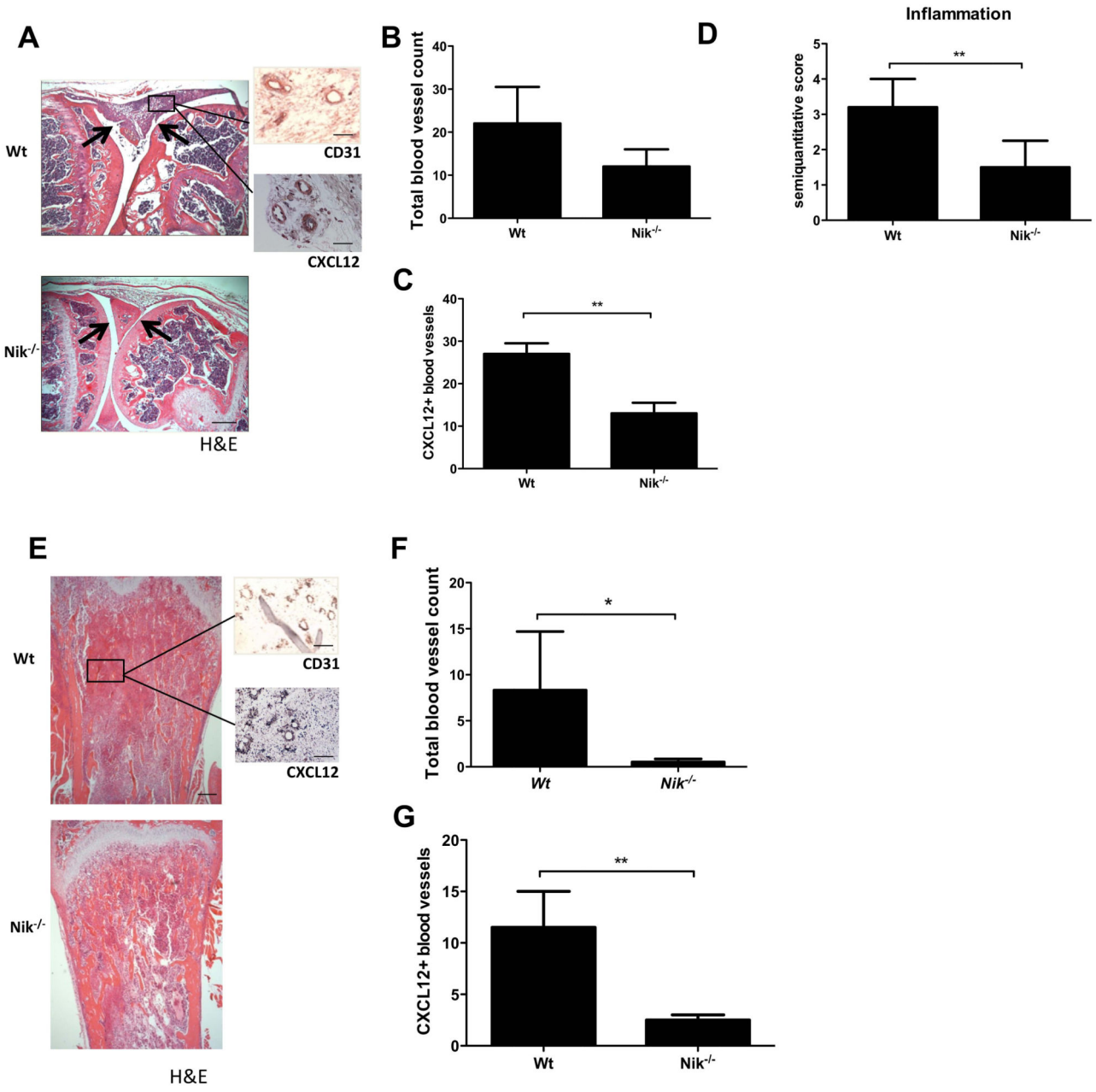

Figure 5. Nik$^{-/-}$ mice exhibit reduced inflammation-induced angiogenesis in arthritis and reduced tumor-associated angiogenesis in a melanoma model

A, Representative picture of a mBSA-injected Wt mouse knee joint showing a severe inflammatory infiltrate (between arrows), in contrast to a mBSA-injected Nik$^{-/-}$ knee joint showing a reduced inflammatory infiltrate and intact cartilage (between arrows; scale bar 500 μm). Sagittal sections of knee joint with H&E staining and CD31 or CXCL12 IHC staining (insets; scale bars 100 μm). **B,** Quantification of the total number of synovial blood vessels in Wt and Nik$^{-/-}$ mice. **C,** Quantification of CXCL12^{+} blood vessels in synovial tissue of Wt and Nik$^{-/-}$ mice. **D,** Quantification of synovial inflammation on a semiquantitative scale of 0 to 4. **E**, Representative pictures of tibial sections from Wt and

$Nik^{-/-}$ mice, with B16 melanoma tumor tissue in trabecular bone. H&E-stained sections of tibias show marrow replacement by tumor cells beneath the growth plate (scale bar 500 μm), and insets show CD31 and CXCL12 IHC staining on tumor tissue (scale bar insets, 100 μm). **F,** Quantification of the total number of blood vessels in melanoma tumor tissue in Wt and $Nik^{-/-}$ mice. **G,** Quantification of $CXCL12^{+}$ blood vessels in melanoma tumor tissue of Wt and $Nik^{-/-}$ mice. Panels A-D: n=5 per group; Panels E-G: n=6 per group. Panels B-D,F,G represent mean±SEM *<P0.05, **P<0.001.